Prompt-ICM: A Unified Framework towards Image Coding for Machines with Task-driven Prompts

Ruoyu Feng[1*]   Jinming Liu[2*]   Xin Jin[3]   Xiaohan Pan[1] Heming Sun[2]   Zhibo Chen [1,†]

[1]University of Science and Technology of China   [2]Waseda University   [3]Eastern Institute of Advanced Study

Abstract

*Image coding for machines (ICM) aims to compress images to support downstream AI analysis instead of human perception. For ICM, developing a unified codec to reduce information redundancy while empowering the compressed features to support various vision tasks is very important, which inevitably faces two core challenges: 1) How should the compression strategy be adjusted based on the downstream tasks? 2) How to well adapt the compressed features to different downstream tasks? Inspired by recent advances in transferring large-scale pre-trained models to downstream tasks via prompting, in this work, we explore a new ICM framework, termed Prompt-ICM. To address both challenges by carefully learning **task-driven prompts** to coordinate well the compression process and downstream analysis. Specifically, our method is composed of two core designs: a) **compression prompts**, which are implemented as importance maps predicted by an information selector, and used to achieve different content-weighted bit allocations during compression according to different downstream tasks; b) **task-adaptive prompts**, which are instantiated as a few learnable parameters specifically for tuning compressed features for the specific intelligent task. Extensive experiments demonstrate that with a single feature codec and a few extra parameters, our proposed framework could efficiently support different kinds of intelligent tasks with much higher coding efficiency.*

1. Introduction

In modern society, intelligent multimedia applications have played an irreplaceable role in our daily life, such as smart cities, intelligent surveillance, and the Internet of Things (IoT). With the fast development of machine vision technologies, there will be more and more images that need to be compressed and transmitted over the Internet to serve intelligent analysis. One of the key technologies is

---
* First two authors contributed equally.
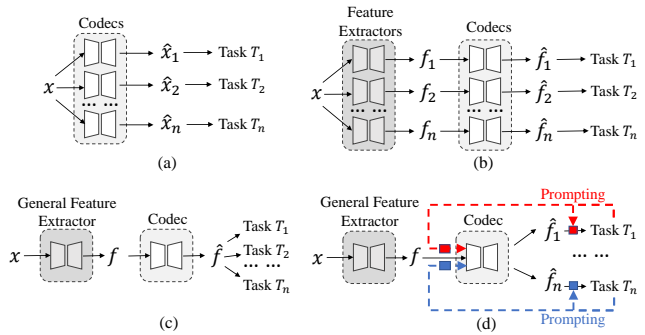† Corresponding author.

Figure 1. Different pipelines of image coding for machines (ICM): (a). Using the compressed images to support downstream tasks; (b). One-to-one feature-based ICM pipeline; (c). General features based ICM pipelines which ignores the explicit interaction between the compression task and downstream tasks. (d). Compared with (c). we further consider using task-driven prompts (those colours) to better coordinate the compression process and downstream analysis.

lossy compression, which aims to save storage resources and transmission bandwidth. In the past decades, hand-crafted image and video codecs [8, 63, 73, 76, 79] have significantly improved coding efficiency.

Recently, learned-based codecs [5,6,16,37,43,44,57–59] have shown strong potential, which not only outperform traditional hand-crafted codecs in PSNR, but also can be optimized according to perception-related metrics (e.g., MS-SSIM [78], LPIPS [84]) to generate more realistic images. However, these codecs are mainly designed to satisfy human perception. When facing AI task analysis, existing image coding methods (even the learned-based ones) are still questionable. Due to the fundamental differences between the information needs of intelligent tasks and human vision, and the existence of various, perhaps even unknown tasks, utilizing existing codecs to compress images for downstream tasks is likely to yield suboptimal outcomes.

Therefore, a new task of compressing images for machine vision, called **image coding for machines (ICM)** [23,40], has emerged to build a joint efficient and analytical framework. Such a framework is capable of obtaining and

compressing general representations to effectively support intelligent analytics for massive and diverse applications.

The existing ICM methods can be divided into three branches: Figure 1 (a) shows the first branch that uses task-specific codecs to compress images [40, 41], and then perform intelligent analysis based on reconstructed images. These codecs are typically optimized for their respective task losses along with rate losses, in an end-to-end manner. As shown in Figure 1 (b), methods in the second branch [2, 14, 15, 24, 25, 56, 71] firstly extract specific features for individual compression, and finally use the reconstructed features to complete the intelligent task analysis. Note that, such two branches have a large limitation: the different intelligent tasks need to use their corresponding codecs for compression, respectively, *i.e.*, lack of generalization. And the lack of generalization might cause a significant extra cost of computation and storage for different downstream tasks. To overcome this defect, the third branch has been explored (as shown in Figure 1 (c) [26]). This method comprises a generic feature extractor and its associated feature codec, which reconstructs the general features for all subsequent tasks. However, it suffers from suboptimal efficiency due to its disregard for task-specific characteristics during compression and downstream analysis. In other words, the potential benefits of an optimized compression scheme tailored to individual downstream tasks have not been fully leveraged.

In this paper, we tend to explore a new framework for image coding for machines (ICM) that circumvents the aforementioned issues. Inspired by the recent successes of parameter efficient tuning for transferring large-scale pretrained models to downstream tasks [10, 36, 60, 83, 87, 88], we design a new ICM framework, termed as Prompt-ICM, from a new aspect of carefully learning task-driven prompts to coordinate well the compression process and downstream analysis, as shown in Figure 1 (d). This framework consists of two core designs. The first design is compression prompts, which refer to importance maps that represent the positional importance distribution conditioned on the extracted features and the corresponding intelligent task. More specifically, the compression prompts are predicted by a lightweight information selector (IS) module and utilized in conjunction with a spatially variable-rate feature compression model to achieve content-weighted bit allocation during the compression process, tailored to the specific task requirements. The second component of our framework is task-adaptive prompts, which incorporate a few additional learnable parameters to analyze the compressed features for the specific downstream task. Together with compression prompts, enabling our Prompt-ICM framework to utilize a unified codec that efficiently supports diverse intelligent tasks with superior compression performance.

The main contributions of this paper are summarised as follows:

- To the best of our knowledge, we are the first to investigate and formulate the coordination of the interaction between compression and downstream analytics in a unified framework. Our proposed Prompt-ICM can support different kinds of intelligent tasks based on only a single codec.

- We propose the compression prompts for content-weighted compression according to the demands of downstream tasks. As a by-product contribution, we design an effective sub-component, a lightweight information selector (IS) module, to predict importance maps as compression prompts.

- Furthermore, we propose task-adaptive prompt tuning to transfer compressed features for downstream tasks, achieving significant performance improvement with a few parameters, which is more practical for ICM applications.

2. Related Work

2.1. Image Compression

Image compression aims to represent original pixel samples using a compact and high-fidelity format. Traditional hand-crafted image codecs typically involve intra prediction, discrete cosine transformation or wavelet transformation, quantization, and entropy coding [8, 63, 73, 76, 79]. Learned-based codecs [5, 6, 16, 37, 43, 44, 57–59] make use of neural networks to learn to minimize distortion between pairs of source images and reconstructed images, while maximizing the likelihood of the quantized latent representation for low bitrate in an end-to-end manner. Furthermore, the utilization of learned-based compression models offers a significant advantage in terms of versatility through the joint optimization of perceptual metrics such as MS-SSIM [78], LPIPS [84], and adversarial loss [58]. Despite a potential decrease in signal fidelity, compression models optimized with these metrics can produce more realistic images. However, since the rate-distortion trade-off is controlled by a Lagrange multiplier λ, most existing methods are limited in that a fixed value of λ corresponds to a single point in the rate-distortion curve. Recent works [17, 20, 37, 74, 82] propose different approaches to support variable rates using a single model. Song *et al.* [72] propose to perform spatial bit allocation according to a quality map that is the same size as the original image.

2.2. Image Coding for Machines

Image coding for machines (ICM) targets at compressing and transmitting source images to support downstream

intelligent tasks, such as image classification [22, 29, 32, 36, 52], object detection [47, 48, 67–69], instance segmentation [7, 31, 51], and semantic segmentation [3, 12, 13, 53, 81, 86]. A natural way is joint optimization [1, 34, 40, 45, 77] of image compression models and the downstream intelligent tasks. Another branch of intuitive methods compresses the features [2, 14, 15, 24, 25, 56, 71] of corresponding tasks instead of images for both coding efficiency and computing offloading. Recently, Feng *et al.* [26] propose to learn features that are both general and compact based on joint optimization of self-supervised learning and entropy constraint. And all intelligent tasks are performed based on the extracted features. Nevertheless, this method doesn't consider the coordination between the compression process and downstream transferring, lacking targeted adjustments for different tasks. Differently, this paper aims to design a unified framework that contains the advantages of the above methods and avoids the corresponding disadvantages. More specifically, we explore the coordination between general feature compression and downstream task transferring and propose a unified framework that can adapt to different kinds of machine vision tasks based on a single compression model with a few learnable parameters.

2.3. Parameter Efficient Tuning for Large-scale Pre-trained Models

Parameter efficient tuning (PET) is first introduced in NLP [30, 33, 42, 46, 50, 62] since it's inefficient to fully fine-tune all parameters of large-scale pre-trained models [9, 35, 64–66] on each downstream intelligent task. In computer vision, parameter efficient tuning is first introduced to large-scale pre-trained visiaon-language models [35, 64] via prompt-based tuning [87, 88], which introduces additional learnable prompts attached to the input during the training stage, while keeping the pre-trained models fixed. Zhang *et al.* [83] and Gao *et al.* [27] design lightweight adapters to predict the adapted feature residuals to modulate representation space. Jia *et al.* [36] adapt visual prompts for supervised pre-trained vision transformers. Bahng *et al.* [4] explore visual prompts in input pixel space for adapting pre-trained models. Nie *et al.* [60] inserts several lightweight prompt blocks into backbones to adjust feature representation. This paper considers a more practical scenario of multiple downstream intelligent tasks supported for ICM. In combination with PET methods, our framework can support different downstream tasks more efficiently.

3. Approach

3.1. Formulation of General ICM

In this section, we mathematically define the problem of general ICM from a new perspective, which is formu-

lated by Equation (1)-(4). To begin with, the input image x is firstly analyzed by the pre-trained feature extractor FE_i with parameters θ_{FE_i} to extract the feature f_i for task i:

$$f_i = FE_i\left(x; \theta_{FE_i}\right). \tag{1}$$

Note that when FE_i is None, f_i refers to the raw image x for subsequent operations, as Figure 1 (a) shows.

After that, a lossy codec C_i with parameters θ_{C_i} is used to compress the features f_i for task i:

$$\hat{f}_i = C_i\left(f_i; \theta_{C_i}\right). \tag{2}$$

Then the reconstructed feature $\hat{f}_i$ is sent to the remaining networks T_i with parameters θ_{T_i} to acquire prediction results o_i:

$$o_i = T_i\left(\hat{f}_i; \theta_{T_i}\right). \tag{3}$$

Generally, the optimization function of the ICM framework for downstream transferring can be described as:

$$argmin_{\Phi=\left\{\theta_{FE_i}, \theta_{C_i}, \theta_{T_i}\right\}} \alpha \mathcal{L}_i + R. \tag{4}$$

where the Lagrange multiplier α controls the trade-off between bitrate R and loss $\mathcal{L}_i$ for task i.

3.2. Overview

In contrast to general ICM, we propose a new ICM framework called Prompt-ICM. Firstly, similar to Figure 1 (c), we use a single **general feature extractor** with fixed parameters φ_{FE} to extract the general feature for all downstream tasks instead of extracting different features for different tasks. The Equation (1) in our framework can be revised as follows:

$$f = FE\left(x; \varphi_{FE}\right). \tag{5}$$

This will significantly reduce the extra cost of computation and storage for different downstream tasks.

However, the framework corresponding to Figure 1 (c) does not take into account the task-specific characteristics during compression, which may result in inefficient coding for specific tasks. To mitigate the aforementioned issue, we propose a lightweight information selector module (IS) with tunable parameters θ_{IS}. The module generates importance maps as **compression prompts**, which are used to guide the spatial bit allocation of the codec. The general feature extractor and customized compression prompts enable us to employ a single controllable feature codec C with parameters φ_C for all various downstream tasks instead of designing distinct codecs for different tasks. Therefore, Equation (2) in our framework can be revised as:

$$m_i = IS_i\left(f; \theta_{IS_i}\right). \tag{6}$$

In this paper, we use θ to represent learnable parameters, while using φ to represent fixed parameters for downstream tasks.
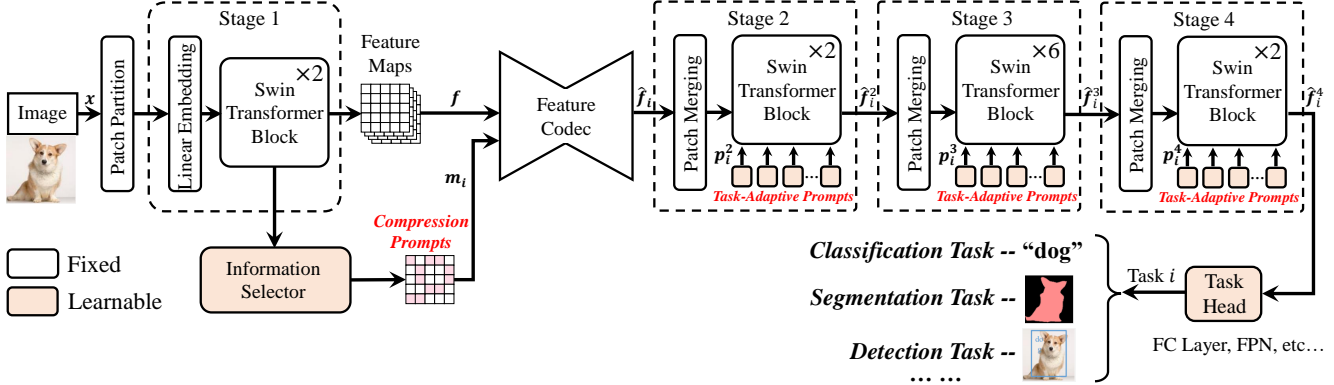
Figure 2. The framework of our proposed Prompt-ICM (taking Swin-T as an example). Downstream transferring is performed via task-driven prompt tuning. By tuning the lightweight information selector and task-adaptive prompts, Prompt-ICM could efficiently support various downstream tasks, e.g., classification, segmentation, and detection.

$$\hat{\boldsymbol{f}}_i = \boldsymbol{C}\left(\boldsymbol{f}, \boldsymbol{m}_i; \varphi_{\boldsymbol{C}}\right). \tag{7}$$

The next step is to send the reconstructed feature $\hat{\boldsymbol{f}}_i$ to $\boldsymbol{T}_i$ to acquire prediction. Nevertheless, fine-tuning $\boldsymbol{T}_i$ for each downstream task is parameter-consuming. In this paper, we utilize the **task-adaptive prompts** $\boldsymbol{p}_i$ with a few learnable parameters $\theta_{\boldsymbol{p}_i}$ to conduct efficient transferring. Then the Equation (3) in our framework can be revised as follows:

$$o_i = \boldsymbol{T}_i\left(\hat{\boldsymbol{f}}_i, \boldsymbol{p}_i; \varphi_{\boldsymbol{T}'_i}, \theta_{\boldsymbol{p}_i}, \theta_{\boldsymbol{h}_i}\right). \tag{8}$$

where the parameters of $\boldsymbol{T}_i$ are divided to two parts: $\theta_{\boldsymbol{h}_i}$ denotes the parameters of the task head, while remaining fixed parameters are represented as $\varphi_{\boldsymbol{T}'_i}$.

Notably, when transferring to downstream tasks, we only need to fine-tune the information selector, the task head, and task-adaptive prompts. The optimization function can be revised as follows:

$$argmin_{\Phi' = \left\{\theta_{\boldsymbol{IS}_i}, \theta_{\boldsymbol{h}_i}, \theta_{\boldsymbol{p}_i}\right\}} \alpha \mathcal{L}_i + R, \tag{9}$$

where the number of trainable parameters Φ' in Equation (9) is far fewer than Φ in Equation (4).

3.3. General Feature Extraction

With a large-scale pre-trained vision model, the whole network is first divided into multiple sub-layers as stages. We follow the regular concepts of stage partitioning [32, 52]. Considering that the features would be consumed by a variety of kinds of intelligent tasks, *e.g.*, image classification, object detection, and semantic segmentation, the features extracted at stage 1 (with a 4x down-sampling factor) are taken as the general features to promise completeness of information and integrity of the content's spatial layout. Formally, consider s_1 to be the first stage of a pre-trained vision model $\boldsymbol{S} = \{s_j\}_{j=1}^n$ with n-stages.

(a)

(b)

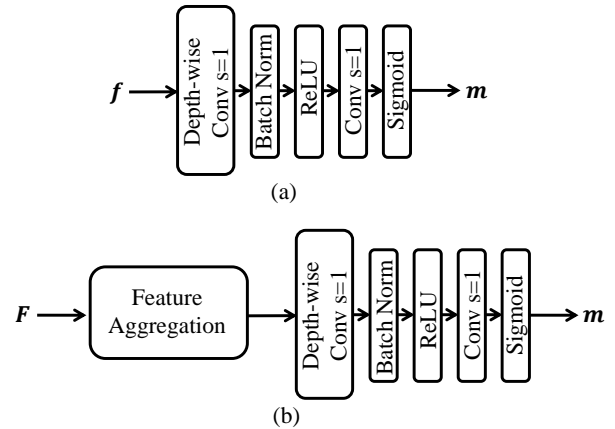Figure 3. Two variants of information selector modules that differ in the input features for generating compression prompts.

Given an input image $\boldsymbol{x}$, we feed it into s_1 to obtain the feature map $\boldsymbol{f}$ with $4\times$ down-sampling, i.e., $\boldsymbol{FE} = s_1$.

In this paper, we take the Swin Transformer [52] as the base model for its strong representation capability and functionalities resulting from the hierarchical design.

3.4. Compression Prompts

During each inference, we use compression prompts $\boldsymbol{m}$ generated by a lightweight information selector ($\boldsymbol{IS}$) to guide content-weighted feature compression corresponding to the current task.

Generation of Compression Prompts. As shown in Figure 3 (a), $\boldsymbol{IS}$ module is used to extract importance maps as compression prompts. Besides, we can perform additional forward propagation at the encoding side to obtain multi-scale features $\boldsymbol{F} = \{\boldsymbol{f}^k\}_{k=1}^n$ which contain richer and hierarchical information. Note that $\boldsymbol{f}^1$ in $\boldsymbol{F}$ corresponds to $\boldsymbol{f}$ in Section 3.3. Then, the Equation (6) can be revised as $\boldsymbol{m}_i = \boldsymbol{IS}_i\left(\boldsymbol{F}; \theta_{\boldsymbol{IS}_i}\right)$. And the $\boldsymbol{IS}$ module can aggregate

these features from multiple semantic levels to better generate compression prompts, as shown in Figure 3 (b).

Content-weighted Feature Compression. To make use of the compression prompts, we design a controllable feature codec by adjusting previous learned lossy compression methods to enable compression prompts $\boldsymbol{m}_i$ to guide content-weighted feature compression for task i. Notably, to ensure the irrelevance of any specific task, the training of the codec is independent of the rest of the network in the whole framework.

In previously learned lossy image compression, the goal is to simultaneously minimize the bitrate and the distortion. Such an objective can be formulated as minimizing:

$$R + \lambda D. \tag{10}$$

where R represents the bitrate, D denotes the distortion between the original features and the reconstructed features, and λ is the Lagrange multiplier that controls the rate-distortion trade-off. In our framework, we go beyond previous learned-based codecs in that one model controlled by a fixed value of λ corresponds to a single point in the rate-distortion curve, and build a feature codec that can conduct bit allocation according to manually set compression prompts $\boldsymbol{m}$. Thus the Equation (10) is newly written as:

$$R + \boldsymbol{\Lambda} \cdot \boldsymbol{D}, \tag{11}$$

where $\boldsymbol{\Lambda} = \{\lambda_{h,w}\}_{h=1,w=1}^{H,W}$ denotes the importance of each position, and $\boldsymbol{\Lambda} = \boldsymbol{m}$. $\boldsymbol{D} = \{D_{h,w}\}_{h=1,w=1}^{H,W}$ represents the distortion in each position of the feature $\boldsymbol{f}$ and the reconstructed feature $\hat{\boldsymbol{f}}$.

More specifically, we design the compression framework derived from the Mean & Scale (M&S) Hyperprior model [59] and spatial variable-rate image compression [72]. Since round-based quantization is non-differential, the additive uniform noise [5] is added to the latent variables for rate estimation during training.

The overall R-D (rate-distortion) loss function for the training of the codec is formulated as:

$$
\begin{aligned}
\mathcal{L}_f =& \mathcal{R}(\hat{\boldsymbol{y}}) + \mathcal{R}(\hat{\boldsymbol{z}}) + \boldsymbol{\Lambda} \cdot \boldsymbol{D}(\boldsymbol{f}, \hat{\boldsymbol{f}}) \\
=& \mathbb{E}[-\log_2(p_{\hat{\boldsymbol{y}}|\hat{\boldsymbol{z}}}(\hat{\boldsymbol{y}}|\hat{\boldsymbol{z}}))] + \mathbb{E}[-\log_2(p_{\hat{\boldsymbol{z}}|\boldsymbol{\psi}}(\hat{\boldsymbol{z}}|\boldsymbol{\psi}))] \\
&+ \sum_{h=1}^{H} \sum_{w=1}^{W} \lambda_{h,w} \frac{(f_{h,w} - \hat{f}_{h,w})^2}{HW},
\end{aligned}
\tag{12}
$$

where $p_{\hat{\boldsymbol{y}}|\hat{\boldsymbol{z}}}(\hat{\boldsymbol{y}}|\hat{\boldsymbol{z}})$ denotes the probability distribution of the latent variable $\hat{\boldsymbol{y}}$ which is a compact representation of $\boldsymbol{f}$ and generated by the encoder of the codec. $\hat{\boldsymbol{y}}$ and side information $\hat{\boldsymbol{z}}$ which provides hyper-prior information for $\hat{\boldsymbol{y}}$ are encoded as bitstreams for transmission and storage. The decoded bitstreams are used to generate the reconstructed feature $\hat{\boldsymbol{f}}$. $p_{\hat{\boldsymbol{z}}|\boldsymbol{\psi}}(\hat{\boldsymbol{z}}|\boldsymbol{\psi})$ denotes the probability distribution of side information $\hat{\boldsymbol{z}}$, $\boldsymbol{\psi}$ denotes the factorized density model

to encode $\hat{\boldsymbol{z}}$, H and W denote the height and width of the feature, and $\lambda_{h,w}$ denotes the Lagrange multiplier of the corresponding position. The detailed network architecture, compression process, and formulations are reported in the supplementary.

After the training stage of the feature codec, its parameters are fixed. When transferring to downstream task i, the task-oriented adjustment is achieved by fine-tuning the lightweight $\boldsymbol{IS}_i$ for generating $\boldsymbol{m}_i$, resulting in a unified codec for various intelligent tasks.

3.5. Task-adaptive Prompts

Task-adaptive prompts are instantiated as a few learnable parameters specifically for tuning compressed features for image analysis. They are injected into the pre-trained models on the decoder side, and fine-tuned to fit the specific downstream tasks. It should be noted that the parameters of task-adaptive prompts are much smaller than those of the original task model.

As Figure 2 shows, after obtaining the reconstructed feature $\hat{\boldsymbol{f}}_i$ of task i, task-adaptive prompts $\boldsymbol{p}_i = \{\boldsymbol{p}_i^k\}_{k=2}^n$ are introduced to adjust features during the forward propagation in the rest n-1 stages, corresponding to Equation (8).

The overall loss function for transferring to downstream task i is given by:

$$\mathcal{L} = \mathcal{R}(\hat{\boldsymbol{y}}) + \mathcal{R}(\hat{\boldsymbol{z}}) + \alpha \mathcal{L}_i(o_i, gt_i), \tag{13}$$

where the $\mathcal{R}(\hat{\boldsymbol{y}})$ and $\mathcal{R}(\hat{\boldsymbol{z}})$ denote rate of the latent variables $\hat{\boldsymbol{y}}$ and side information $\hat{\boldsymbol{z}}$, $\mathcal{L}_i(\cdot, \cdot)$, o_i, and gt_i denote the loss function, output, and ground truth of the current task, respectively, and α is the Lagrange multiplier to achieve the trade-off between the task loss and bitrates. Note that in the downstream transferring, only parameters of the information selector, task-adaptive prompts, and the task head are learnable, while the feature extractor, feature compression model, and pre-trained stages are all fixed, thus achieving efficient downstream task transferring.

Thanks to compression prompts for content-weighted information selection and task-adaptive prompt tuning, Prompt-ICM achieves both coding efficiency and parameter efficiency for the downstream transfer to heterogeneous tasks with only a single feature codec, resulting in a simple yet unified framework for image coding for machines.

4. Experiments

4.1. Datasets

For training of the feature codec, we use ImageNet [21] as the training database. As for the verification of downstream task transferring, we experiment on four image classification datasets and two dense prediction datasets. The four image classification datasets are CUB-200-2011 [75], Stanford Dogs [38], Stanford Cars [28], and Oxford Flowers [61], respectively. The two datasets for dense prediction
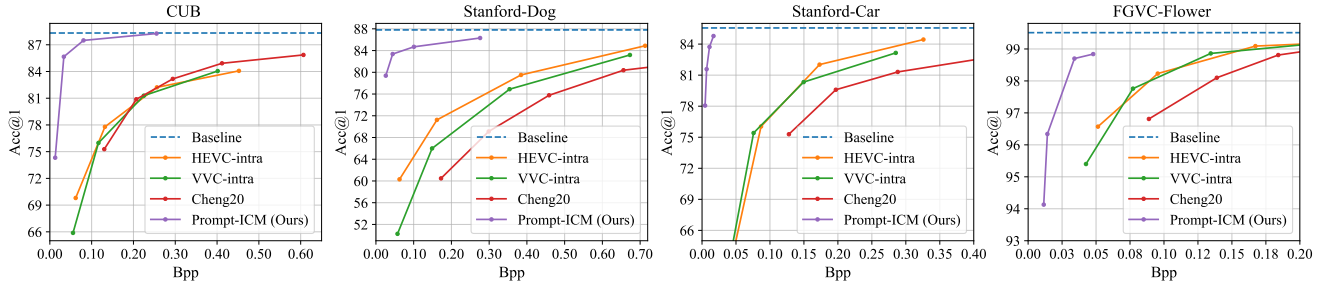
Figure 4. Classification results on different datasets at various bitrates. Two traditional codecs HEVC-intra [73], VVC-intra [8], and one learned-based codec *Cheng20* [16] are compared with our method.
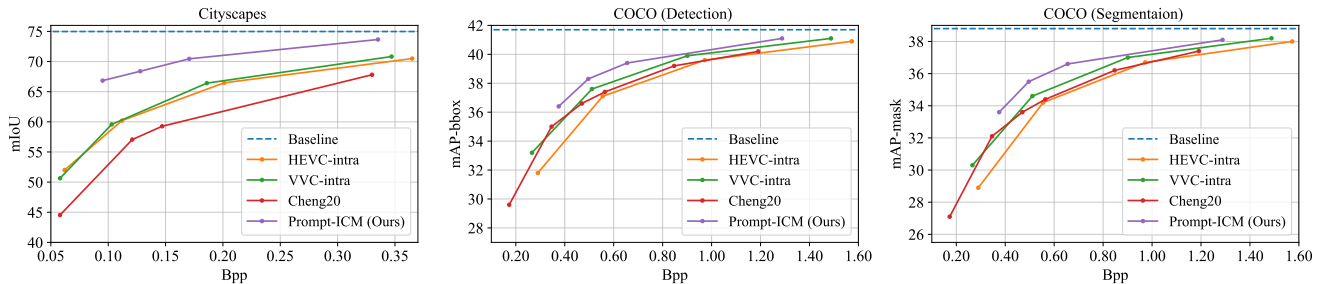

Figure 5. Results of semantic segmentation on Cityscapes (the first one) and object detection and instance segmentation on COCO 2017 (second and third).
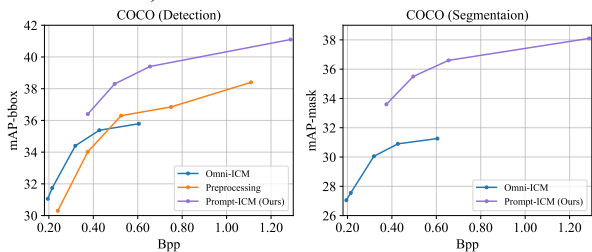

Figure 6. Comparisons with SOTA ICM methods in terms of object detection and instance segmentation on COCO 2017.

are COCO 2017 [49] and Cityscapes [19]. COCO 2017 is a dataset for dense prediction tasks of object detection and instance segmentation that contains 118K training images, 5K validation images, and 20K test-dev images. Cityscapes is a fundamental and challenging dataset, specifically for semantic segmentation. It has 5,000 high-quality images with pixel-level annotations in total, with 2975 for training, 500 for validation, and 1525 for testing, respectively.

4.2. Implementation Details

Large-scale Pre-trained Backbones. We performed experiments using the Swin Transformer [52] model pretrained on the ImageNet-21K dataset [21]. For image classification experiments, we used the Swin-Base model, while for dense prediction experiments, we used the Swin-Tiny model. Additionally, we conducted experiments using the Vision Transformer (ViT) [22], and the results are included in the supplementary.

Controllable Feature Compression. We train the controllable feature codec for 2M iterations with a batch size of 8. Adam [39] optimizer is employed, and the learning rate is 3e-5 and decreases to 3e-6 after 1.8M iterations. The manually set compression prompts m, i.e., Λ in Equation (12) is uniformly sampled from [0.5, 32], resulting in a bpp range of [0.02, 1.0] on the Kodak dataset. During the training stage of the codec, to ensure the variety of possible compression prompts, we randomly generate each instance in a mini-batch by using one of the four different ways (1) a uniform map (2) a gradation map between two randomly selected values (3) a kernel density estimation map of a Gaussian mixture with random mean, variance, and a number of mixtures (4) a map consisting of various blocks in a grid manner.

Downstream Transferring via Task-Driven Prompt Tuning. For compression prompts, we take multi-scale feature aggregation as input to the information selector by default. For task-adaptive prompts, visual prompt tuning (VPT) [36] is instantiated for image classification, and Pro-Tuning [60] is instantiated for dense prediction, *i.e.* object detection, instance segmentation, and semantic segmentation. We follow the default settings in their original papers.

4.3. Effectiveness and Superiority

Evaluation Protocol. We evaluate the rate-distortion performance across various intelligent tasks. The distortion component is represented by metrics specific to each task. The rate component is determined by bits per pixel (bpp),

Table 1. The comparison of learnable parameters between the method of Prompt-ICM and the method of full tuning on different tasks.

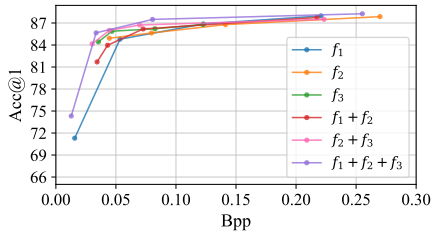| Trainable Parmeters (M)	Cla. (Swin-B)	Det. & Ins. (Swin-T)	Sem. (Swin-T)
Full Tuning	87.61	47.49	59.64
Prompt-ICM	0.87	25.31	37.46

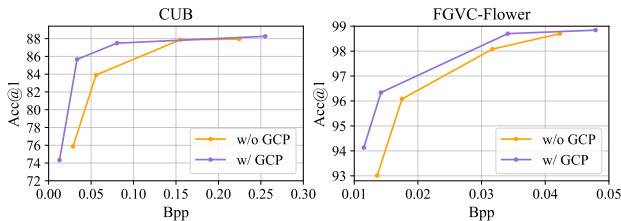Figure 7. Ablation studies on generation of compression prompts using features of different stages.

Figure 8. Ablation studies on generated compression prompts (GCP) based on different datasets. "w/ GCP" represents using generated compression prompts to guide content-weighted coding, while "w/o GCP" refers to the coding with manual compression prompts and cannot allocate bits adaptively.

which is computed as $\frac{b}{h \times w}$, where h and w denote the height and width of the source image, respectively, and b refers to the total bits utilized by the coded feature bitstream.

Comparison Approaches. We mainly compare our method with the most advanced codecs, including traditional codecs (HEVC [73], VVC [8]) and a learned-based codec *Cheng20* [16]. We take the results obtained by feeding uncompressed raw images into the task model as the baseline, or said, performance upper bound. For all subsequent evaluations of the compared approaches, reconstructed images are fed into the task model, which has been previously trained with uncompressed raw images, to obtain the corresponding results.

Image Classification. For training, we follow the default optimization settings in [36]. When evaluating classification tasks, we resize and crop each input image to 224×224 before inputting them into the model. As shown in Figure 4, the R-D performance of our method exceeds compared methods by a significant margin. Surprisingly, our method can perform well at extremely low bitrates (0.03~0.1 bpp). Meanwhile, as shown in Table 1, Prompt-ICM only requires 0.87M learnable parameters to be updated during transferring, while the full-tuning scheme requires 87.61M learn-
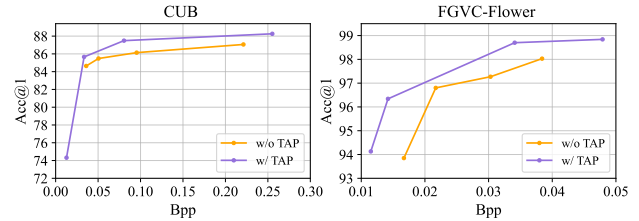

Figure 9. Ablation studies on task-adaptive prompts (TAP). "w/o TAP" corresponds to fully tuning all parameters of pre-trained backbones and the task head on the decoder side.

able parameters. Last but not least, all results of Prompt-ICM are achieved by a unified feature codec, which is critical to practical application scenarios.

Dense Prediction. For semantic segmentation on Cityscapes, we utilize UperNet [80] implemented in mmseg [18] as the base framework. AdamW [54] optimizer with the learning rate of 6e-5 and a weight decay of 0.01 is employed. We use a batch size of 16 for 80K training iterations with the crop size of 512×512. For object detection and instance segmentation tasks on COCO 2017, Mask R-CNN [31] with FPN [85] is utilized as the detector implemented in mmdet [11]. We follow the common protocol that the image scale is in [800, 1333] pixels during both the training and inference stages by default. AdamW [54] optimizer (initial learning rate of 1e-4, weight decay of 0.05, and batch size of 16) is used with 12 epochs. As shown in Figure 5, Prompt-ICM outperforms all other methods on the three dense prediction tasks. Thanks to the conditional compression prompts that help with the content-weighted compression process, Prompt-ICM can allocate more bits to those task-related regions for the dense prediction tasks, which is further confirmed in Section 4.5. Meanwhile, as shown in Table 1, the required numbers of learnable parameters for object detection and instance segmentation, and semantic segmentation are 25.31M and 37.46M, while those of full tuning are 47.49M and 59.64M. It shows that our task-adaptive prompts enable the proposed Prompt-ICM framework to achieve significant parameter savings when transferring to dense prediction tasks.

Comparison with SOTA ICM Methods. We compare our proposed method with Omni-ICM [26] and preprocessing scheme [55], which also only use a single codec for completing ICM tasks. As shown in Figure 6, our method achieves the best performance and significantly outperforms others with much fewer learnable parameters. Additional comparisons on other datasets are reported in the supplementary due to limited space.

4.4. Ablation Study

4.4.1 Study on Compression Prompts

Generation of Compression Prompts. We study the effect of various combinations of features for generating com-

(a) Image classification (b) Object detection (c) Semantic segmentation
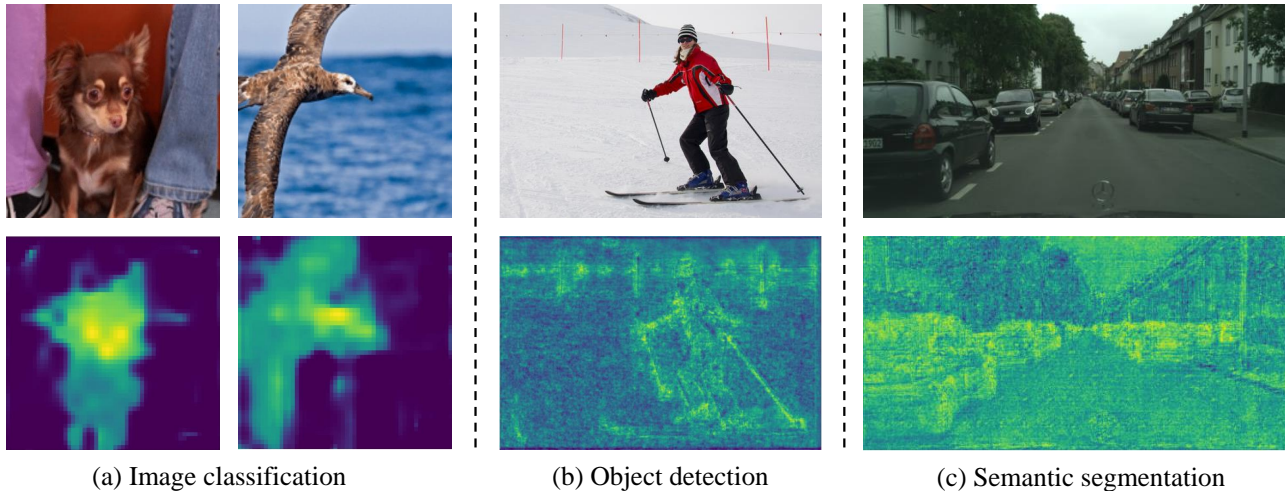
Figure 10. Visualisation results of compression prompts on different tasks, including image classification, object detection, and semantic segmentation. Positions with higher brightness in the compression prompts mean that they are more important.

pression prompts on the classification of the CUB-200-2011 dataset. As illustrated in Figure 7, it can be inferred that the inclusion of all features from stage 1 to stage 3 results in the most superior performance. This observation implies that information derived from multiple semantic levels is advantageous for localizing importance. Moreover, the results indicate that the performance remains relatively stable regardless of the feature combination employed. Thus, the choice of a particular combination should be based on the available computing power and specific requirements to balance the trade-off between performance and complexity.

Content-weighted Feature Compression. To verify that our generated compression prompts adaptively conduct content-weighted feature compression for a specific task, we compare our method to the scheme without using the generated compression prompts. By manually setting the compression prompts to a value between 0 and 1 instead of the compression prompts generated by the information selector, we can implement a codec without information selection. Figure 8 shows that our generated compression prompts lead to a significant improvement in rate-distortion performance on different datasets.

4.4.2 Study on Task-adaptive Prompts

Figure 9 further presents the ablation study about task-adaptive prompts. Combined with the study on learnable parameters shown in Table 1, we can infer that task-adaptive prompt tuning achieves even better performances than the scheme of full tuning (w/o TAP), while tuning the task-adaptive prompts only needs a few parameters (0.87M for task-adaptive prompt tuning vs. 87.61M for full tuning) to be updated during downstream transferring. These findings further provide evidence that our proposed Prompt-ICM approach possesses excellent properties of both coding effi-

ciency and parameter efficiency.

4.5. Vision Analysis and Insights

We visualize the compression prompts for different tasks as shown in Figure 10. It can be inferred that compression prompts are mainly concentrated on objects and edges that are closely related to the current task. During the compression process, compression prompts instruct the codec to allocate more bits to those important regions and fewer bits to less important ones. More specifically, for the classification task, heads of dogs and birds are more critical to classification results, while human legs, regions of road, trees, and the sea are unimportant to task inference. This phenomenon is reasonable and intuitive. For dense prediction tasks, including semantic segmentation and object detection tasks, the importance is broader and more concentrated on the boundaries of objects, which are essential to precise localization and identification. By jointly observing the visualization results of different tasks, it can be inferred that the information selector pays different degrees of attention to tasks of different granularities, pays more attention to discriminative patterns for image-level tasks, and pays more attention to local details for dense prediction tasks.

5. Conclusion

We present Prompt-ICM, a unified framework that makes use of large-scale pre-trained models to support a variety of downstream intelligent tasks. By introducing compression prompts to guide feature compression and task-adaptive prompts for compressed feature tuning, Prompt-ICM can well transfer to different intelligent tasks based on only one feature codec. Our experiments demonstrate the significant superiority of our framework in a wide range of vision-intelligent tasks.

References

[1] Mohammad Akbari, Jie Liang, and Jingning Han. Dsslic: Deep semantic segmentation-based layered image compression. In *ICASSP 2019-2019 IEEE International Conference on Acoustics, Speech and Signal Processing (ICASSP)*, pages 2042–2046. IEEE, 2019. 3

[2] Artem Babenko, Anton Slesarev, Alexandr Chigorin, and Victor Lempitsky. Neural codes for image retrieval. In *ECCV*, pages 584–599. Springer, 2014. 2, 3

[3] Vijay Badrinarayanan, Alex Kendall, and Roberto Cipolla. Segnet: A deep convolutional encoder-decoder architecture for image segmentation. *TPAMI*, 39(12):2481–2495, 2017. 3

[4] Hyojin Bahng, Ali Jahanian, Swami Sankaranarayanan, and Phillip Isola. Exploring visual prompts for adapting large-scale models. *arXiv preprint arXiv:2203.17274*, 1(3):4, 2022. 3

[5] Johannes Ballé, Valero Laparra, and Eero P Simoncelli. End-to-end optimized image compression. In *ICLR*, 2017. 1, 2, 5, 12

[6] Johannes Ballé, David Minnen, Saurabh Singh, Sung Jin Hwang, and Nick Johnston. Variational image compression with a scale hyperprior. In *ICLR*, 2018. 1, 2

[7] Daniel Bolya, Chong Zhou, Fanyi Xiao, and Yong Jae Lee. Yolact: Real-time instance segmentation. In *ICCV*, pages 9157–9166, 2019. 3

[8] Benjamin Bross, Ye-Kui Wang, Yan Ye, Shan Liu, Jianle Chen, Gary J Sullivan, and Jens-Rainer Ohm. Overview of the versatile video coding (vvc) standard and its applications. *TCSVT*, 2021. 1, 2, 6, 7

[9] Tom Brown, Benjamin Mann, Nick Ryder, Melanie Subbiah, Jared D Kaplan, Prafulla Dhariwal, Arvind Neelakantan, Pranav Shyam, Girish Sastry, Amanda Askell, et al. Language models are few-shot learners. *NeurIPS*, 33:1877–1901, 2020. 3

[10] Hao Chen, Ran Tao, Han Zhang, Yidong Wang, Wei Ye, Jindong Wang, Guosheng Hu, and Marios Savvides. Convadapter: Exploring parameter efficient transfer learning for convnets. *arXiv preprint arXiv:2208.07463*, 2022. 2

[11] Kai Chen, Jiaqi Wang, Jiangmiao Pang, Yuhang Cao, Yu Xiong, Xiaoxiao Li, Shuyang Sun, Wansen Feng, Ziwei Liu, Jiarui Xu, Zheng Zhang, Dazhi Cheng, Chenchen Zhu, Tianheng Cheng, Qijie Zhao, Buyu Li, Xin Lu, Rui Zhu, Yue Wu, Jifeng Dai, Jingdong Wang, Jianping Shi, Wanli Ouyang, Chen Change Loy, and Dahua Lin. MMDetection: Open mmlab detection toolbox and benchmark. *arXiv preprint arXiv:1906.07155*, 2019. 7

[12] Liang-Chieh Chen, George Papandreou, Iasonas Kokkinos, Kevin Murphy, and Alan L Yuille. Deeplab: Semantic image segmentation with deep convolutional nets, atrous convolution, and fully connected crfs. *TPAMI*, 40(4):834–848, 2017. 3

[13] Liang-Chieh Chen, Yukun Zhu, George Papandreou, Florian Schroff, and Hartwig Adam. Encoder-decoder with atrous separable convolution for semantic image segmentation. In *ECCV*, pages 801–818, 2018. 3

[14] Zhuo Chen, Kui Fan, Shiqi Wang, Lingyu Duan, Weisi Lin, and Alex Chichung Kot. Toward intelligent sensing: Intermediate deep feature compression. *TIP*, 29:2230–2243, 2019. 2, 3

[15] Zhuo Chen, Kui Fan, Shiqi Wang, Ling-Yu Duan, Weisi Lin, and Alex Kot. Lossy intermediate deep learning feature compression and evaluation. In *ACM MM*, pages 2414–2422, 2019. 2, 3

[16] Zhengxue Cheng, Heming Sun, Masaru Takeuchi, and Jiro Katto. Learned image compression with discretized gaussian mixture likelihoods and attention modules. In *CVPR*, pages 7939–7948, 2020. 1, 2, 6, 7, 12

[17] Yoojin Choi, Mostafa El-Khamy, and Jungwon Lee. Variable rate deep image compression with a conditional autoencoder. In *ICCV*, pages 3146–3154, 2019. 2

[18] MMSegmentation Contributors. MMSegmentation: Openmmlab semantic segmentation toolbox and benchmark. https://github.com/open-mmlab/mmsegmentation, 2020. 7

[19] Marius Cordts, Mohamed Omran, Sebastian Ramos, Timo Rehfeld, Markus Enzweiler, Rodrigo Benenson, Uwe Franke, Stefan Roth, and Bernt Schiele. The cityscapes dataset for semantic urban scene understanding. In *CVPR*, pages 3213–3223, 2016. 6

[20] Ze Cui, Jing Wang, Bo Bai, Tiansheng Guo, and Yihui Feng. G-vae: A continuously variable rate deep image compression framework. *arXiv preprint arXiv:2003.02012*, 2020. 2

[21] Jia Deng, Wei Dong, Richard Socher, Li-Jia Li, Kai Li, and Li Fei-Fei. Imagenet: A large-scale hierarchical image database. In *CVPR*, pages 248–255. Ieee, 2009. 5, 6

[22] Alexey Dosovitskiy, Lucas Beyer, Alexander Kolesnikov, Dirk Weissenborn, Xiaohua Zhai, Thomas Unterthiner, Mostafa Dehghani, Matthias Minderer, Georg Heigold, Sylvain Gelly, et al. An image is worth 16x16 words: Transformers for image recognition at scale. *ICLR*, 2020. 3, 6, 14

[23] Lingyu Duan, Jiaying Liu, Wenhan Yang, Tiejun Huang, and Wen Gao. Video coding for machines: A paradigm of collaborative compression and intelligent analytics. *TIP*, 29:8680–8695, 2020. 1

[24] Ling-Yu Duan, Vijay Chandrasekhar, Jie Chen, Jie Lin, Zhe Wang, Tiejun Huang, Bernd Girod, and Wen Gao. Overview of the mpeg-cdvs standard. *TIP*, 25(1):179–194, 2015. 2, 3

[25] Ling-Yu Duan, Yihang Lou, Yan Bai, Tiejun Huang, Wen Gao, Vijay Chandrasekhar, Jie Lin, Shiqi Wang, and Alex Chichung Kot. Compact descriptors for video analysis: The emerging mpeg standard. *IEEE MultiMedia*, 26(2):44–54, 2018. 2, 3

[26] Ruoyu Feng, Xin Jin, Zongyu Guo, Runsen Feng, Yixin Gao, Tianyu He, Zhizheng Zhang, Simeng Sun, and Zhibo Chen. Image coding for machines with omnipotent feature learning. In *ECCV*, pages 510–528. Springer, 2022. 2, 3, 7, 12, 13

[27] Peng Gao, Shijie Geng, Renrui Zhang, Teli Ma, Rongyao Fang, Yongfeng Zhang, Hongsheng Li, and Yu Qiao. Clip-adapter: Better vision-language models with feature adapters. *arXiv preprint arXiv:2110.04544*, 2021. 3, 13

[28] Timnit Gebru, Jonathan Krause, Yilun Wang, Duyun Chen, Jia Deng, and Li Fei-Fei. Fine-grained car detection for visual census estimation. In *AAAI*, volume 31, 2017. 5, 14

[29] Kai Han, An Xiao, Enhua Wu, Jianyuan Guo, Chunjing Xu, and Yunhe Wang. Transformer in transformer. *NeurIPS*, 34:15908–15919, 2021. 3

[30] Junxian He, Chunting Zhou, Xuezhe Ma, Taylor Berg-Kirkpatrick, and Graham Neubig. Towards a unified view of parameter-efficient transfer learning. *ICLR*, 2021. 3

[31] Kaiming He, Georgia Gkioxari, Piotr Dollár, and Ross Girshick. Mask r-cnn. In *ICCV*, pages 2961–2969, 2017. 3, 7

[32] Kaiming He, Xiangyu Zhang, Shaoqing Ren, and Jian Sun. Deep residual learning for image recognition. In *CVPR*, pages 770–778, 2016. 3, 4

[33] Neil Houlsby, Andrei Giurgiu, Stanislaw Jastrzebski, Bruna Morrone, Quentin De Laroussilhe, Andrea Gesmundo, Mona Attariyan, and Sylvain Gelly. Parameter-efficient transfer learning for nlp. In *ICML*, pages 2790–2799. PMLR, 2019. 3

[34] Yueyu Hu, Shuai Yang, Wenhan Yang, Ling-Yu Duan, and Jiaying Liu. Towards coding for human and machine vision: A scalable image coding approach. In *2020 IEEE International Conference on Multimedia and Expo (ICME)*, pages 1–6. IEEE, 2020. 3

[35] Chao Jia, Yinfei Yang, Ye Xia, Yi-Ting Chen, Zarana Parekh, Hieu Pham, Quoc Le, Yun-Hsuan Sung, Zhen Li, and Tom Duerig. Scaling up visual and vision-language representation learning with noisy text supervision. In *ICML*, pages 4904–4916. PMLR, 2021. 3

[36] Menglin Jia, Luming Tang, Bor-Chun Chen, Claire Cardie, Serge Belongie, Bharath Hariharan, and Ser-Nam Lim. Visual prompt tuning. *ECCV*, 2022. 2, 3, 6, 7, 13, 14

[37] Nick Johnston, Damien Vincent, David Minnen, Michele Covell, Saurabh Singh, Troy Chinen, Sung Jin Hwang, Joel Shor, and George Toderici. Improved lossy image compression with priming and spatially adaptive bit rates for recurrent networks. In *CVPR*, pages 4385–4393, 2018. 1, 2

[38] Aditya Khosla, Nityananda Jayadevaprakash, Bangpeng Yao, and Fei-Fei Li. Novel dataset for fine-grained image categorization: Stanford dogs. In *Proc. CVPR workshop on fine-grained visual categorization (FGVC)*, volume 2. Citeseer, 2011. 5, 14

[39] Diederik P Kingma and Jimmy Ba. Adam: A method for stochastic optimization. *arXiv preprint arXiv:1412.6980*, 2014. 6

[40] Nam Le, Honglei Zhang, Francesco Cricri, Ramin Ghaznavi-Youvalari, and Esa Rahtu. Image coding for machines: An end-to-end learned approach. In *ICASSP 2021-2021 IEEE International Conference on Acoustics, Speech and Signal Processing (ICASSP)*, pages 1590–1594. IEEE, 2021. 1, 2, 3

[41] Nam Le, Honglei Zhang, Francesco Cricri, Ramin Ghaznavi-Youvalari, Hamed Rezazadegan Tavakoli, and Esa Rahtu. Learned image coding for machines: A content-adaptive approach. In *2021 IEEE International Conference on Multimedia and Expo (ICME)*, pages 1–6. IEEE, 2021. 2

[42] Brian Lester, Rami Al-Rfou, and Noah Constant. The power of scale for parameter-efficient prompt tuning. *arXiv preprint arXiv:2104.08691*, 2021. 3

[43] Mu Li, Wangmeng Zuo, Shuhang Gu, Jane You, and David Zhang. Learning content-weighted deep image compression. *TPAMI*, 2020. 1, 2

[44] Mu Li, Wangmeng Zuo, Shuhang Gu, Debin Zhao, and David Zhang. Learning convolutional networks for content-weighted image compression. In *CVPR*, pages 3214–3223, 2018. 1, 2

[45] Xin Li, Jun Shi, and Zhibo Chen. Task-driven semantic coding via reinforcement learning. *TIP*, 2021. 3

[46] Xiang Lisa Li and Percy Liang. Prefix-tuning: Optimizing continuous prompts for generation. *arXiv preprint arXiv:2101.00190*, 2021. 3

[47] Yanghao Li, Hanzi Mao, Ross Girshick, and Kaiming He. Exploring plain vision transformer backbones for object detection. *ECCV*, 2022. 3

[48] Tsung-Yi Lin, Piotr Dollár, Ross Girshick, Kaiming He, Bharath Hariharan, and Serge Belongie. Feature pyramid networks for object detection. In *CVPR*, pages 2117–2125, 2017. 3

[49] Tsung-Yi Lin, Michael Maire, Serge Belongie, James Hays, Pietro Perona, Deva Ramanan, Piotr Dollár, and C Lawrence Zitnick. Microsoft coco: Common objects in context. In *ECCV*, pages 740–755. Springer, 2014. 6

[50] Pengfei Liu, Weizhe Yuan, Jinlan Fu, Zhengbao Jiang, Hiroaki Hayashi, and Graham Neubig. Pre-train, prompt, and predict: A systematic survey of prompting methods in natural language processing. *arXiv preprint arXiv:2107.13586*, 2021. 3

[51] Shu Liu, Lu Qi, Haifang Qin, Jianping Shi, and Jiaya Jia. Path aggregation network for instance segmentation. In *CVPR*, pages 8759–8768, 2018. 3

[52] Ze Liu, Yutong Lin, Yue Cao, Han Hu, Yixuan Wei, Zheng Zhang, Stephen Lin, and Baining Guo. Swin transformer: Hierarchical vision transformer using shifted windows. In *ICCV*, pages 10012–10022, 2021. 3, 4, 6

[53] Jonathan Long, Evan Shelhamer, and Trevor Darrell. Fully convolutional networks for semantic segmentation. In *CVPR*, pages 3431–3440, 2015. 3

[54] Ilya Loshchilov and Frank Hutter. Decoupled weight decay regularization. *arXiv preprint arXiv:1711.05101*, 2017. 7

[55] Guo Lu, Xingtong Ge, Tianxiong Zhong, Jing Geng, and Qiang Hu. Preprocessing enhanced image compression for machine vision. *arXiv preprint arXiv:2206.05650*, 2022. 7

[56] Siwei Ma, Xiang Zhang, Shiqi Wang, Xinfeng Zhang, Chuanmin Jia, and Shanshe Wang. Joint feature and texture coding: Toward smart video representation via front-end intelligence. *TCSVT*, 29(10):3095–3105, 2018. 2, 3

[57] Fabian Mentzer, Eirikur Agustsson, Michael Tschannen, Radu Timofte, and Luc Van Gool. Conditional probability models for deep image compression. In *CVPR*, pages 4394–4402, 2018. 1, 2

[58] Fabian Mentzer, George Toderici, Michael Tschannen, and Eirikur Agustsson. High-fidelity generative image compression. *arXiv preprint arXiv:2006.09965*, 2020. 1, 2

[59] David Minnen, Johannes Ballé, and George Toderici. Joint autoregressive and hierarchical priors for learned image compression. In *NeurIPS*, 2018. 1, 2, 5, 12

[60] Xing Nie, Bolin Ni, Jianlong Chang, Gaomeng Meng, Chunlei Huo, Zhaoxiang Zhang, Shiming Xiang, Qi Tian, and Chunhong Pan. Pro-tuning: Unified prompt tuning for vision tasks. *arXiv preprint arXiv:2207.14381*, 2022. 2, 3, 6, 13

[61] Maria-Elena Nilsback and Andrew Zisserman. Automated flower classification over a large number of classes. In *2008 Sixth Indian Conference on Computer Vision, Graphics & Image Processing*, pages 722–729. IEEE, 2008. 5, 14

[62] Jonas Pfeiffer, Andreas Rücklé, Clifton Poth, Aishwarya Kamath, Ivan Vulić, Sebastian Ruder, Kyunghyun Cho, and Iryna Gurevych. Adapterhub: A framework for adapting transformers. *arXiv preprint arXiv:2007.07779*, 2020. 3

[63] Majid Rabbani and Rajan Joshi. An overview of the jpeg 2000 still image compression standard. *Signal processing: Image communication*, 17(1):3–48, 2002. 1, 2

[64] Alec Radford, Jong Wook Kim, Chris Hallacy, Aditya Ramesh, Gabriel Goh, Sandhini Agarwal, Girish Sastry, Amanda Askell, Pamela Mishkin, Jack Clark, et al. Learning transferable visual models from natural language supervision. In *ICML*, pages 8748–8763. PMLR, 2021. 3

[65] Alec Radford, Karthik Narasimhan, Tim Salimans, Ilya Sutskever, et al. Improving language understanding by generative pre-training. 2018. 3

[66] Alec Radford, Jeffrey Wu, Rewon Child, David Luan, Dario Amodei, Ilya Sutskever, et al. Language models are unsupervised multitask learners. *OpenAI blog*, 1(8):9, 2019. 3

[67] Joseph Redmon, Santosh Divvala, Ross Girshick, and Ali Farhadi. You only look once: Unified, real-time object detection. In *CVPR*, pages 779–788, 2016. 3

[68] Joseph Redmon and Ali Farhadi. Yolo9000: better, faster, stronger. In *CVPR*, pages 7263–7271, 2017. 3

[69] Shaoqing Ren, Kaiming He, Ross Girshick, and Jian Sun. Faster r-cnn: Towards real-time object detection with region proposal networks. *NeurIPS*, 28:91–99, 2015. 3

[70] Jorma Rissanen and Glen Langdon. Universal modeling and coding. *IEEE Transactions on Information Theory*, 27(1):12–23, 1981. 12

[71] Saurabh Singh, Sami Abu-El-Haija, Nick Johnston, Johannes Ballé, Abhinav Shrivastava, and George Toderici. End-to-end learning of compressible features. In *2020 IEEE International Conference on Image Processing (ICIP)*, pages 3349–3353. IEEE, 2020. 2, 3

[72] Myungseo Song, Jinyoung Choi, and Bohyung Han. Variable-rate deep image compression through spatially-adaptive feature transform. In *ICCV*, pages 2380–2389, 2021. 2, 5, 12

[73] Gary J Sullivan, Jens-Rainer Ohm, Woo-Jin Han, and Thomas Wiegand. Overview of the high efficiency video coding (hevc) standard. *TCSVT*, 22(12):1649–1668, 2012. 1, 2, 6, 7

[74] George Toderici, Damien Vincent, Nick Johnston, Sung Jin Hwang, David Minnen, Joel Shor, and Michele Covell. Full resolution image compression with recurrent neural networks. In *CVPR*, pages 5306–5314, 2017. 2

[75] Catherine Wah, Steve Branson, Peter Welinder, Pietro Perona, and Serge Belongie. The caltech-ucsd birds-200-2011 dataset. 2011. 5, 12, 13, 14

[76] Gregory K Wallace. The jpeg still picture compression standard. *IEEE transactions on consumer electronics*, 38(1):xviii–xxxiv, 1992. 1, 2

[77] Shurun Wang, Shiqi Wang, Wenhan Yang, Xinfeng Zhang, Shanshe Wang, Siwei Ma, and Wen Gao. Towards analysis-friendly face representation with scalable feature and texture compression. *TMM*, 2021. 3

[78] Zhou Wang, Alan C Bovik, Hamid R Sheikh, and Eero P Simoncelli. Image quality assessment: from error visibility to structural similarity. *TIP*, 13(4):600–612, 2004. 1, 2

[79] Thomas Wiegand, Gary J Sullivan, Gisle Bjontegaard, and Ajay Luthra. Overview of the h. 264/avc video coding standard. *TCSVT*, 13(7):560–576, 2003. 1, 2

[80] Tete Xiao, Yingcheng Liu, Bolei Zhou, Yuning Jiang, and Jian Sun. Unified perceptual parsing for scene understanding. In *Proceedings of the European conference on computer vision (ECCV)*, pages 418–434, 2018. 7

[81] Enze Xie, Wenhai Wang, Zhiding Yu, Anima Anandkumar, Jose M Alvarez, and Ping Luo. Segformer: Simple and efficient design for semantic segmentation with transformers. *NeurIPS*, 34:12077–12090, 2021. 3

[82] Fei Yang, Luis Herranz, Joost Van De Weijer, José A Iglesias Guitián, Antonio M López, and Mikhail G Mozerov. Variable rate deep image compression with modulated autoencoder. *IEEE Signal Processing Letters*, 27:331–335, 2020. 2

[83] Renrui Zhang, Rongyao Fang, Peng Gao, Wei Zhang, Kunchang Li, Jifeng Dai, Yu Qiao, and Hongsheng Li. Tip-adapter: Training-free clip-adapter for better vision-language modeling. *arXiv preprint arXiv:2111.03930*, 2021. 2, 3

[84] Richard Zhang, Phillip Isola, Alexei A Efros, Eli Shechtman, and Oliver Wang. The unreasonable effectiveness of deep features as a perceptual metric. In *CVPR*, pages 586–595, 2018. 1, 2

[85] Hengshuang Zhao, Jianping Shi, Xiaojuan Qi, Xiaogang Wang, and Jiaya Jia. Pyramid scene parsing network. In *CVPR*, pages 2881–2890, 2017. 7

[86] Sixiao Zheng, Jiachen Lu, Hengshuang Zhao, Xiatian Zhu, Zekun Luo, Yabiao Wang, Yanwei Fu, Jianfeng Feng, Tao Xiang, Philip HS Torr, et al. Rethinking semantic segmentation from a sequence-to-sequence perspective with transformers. In *CVPR*, pages 6881–6890, 2021. 3

[87] Kaiyang Zhou, Jingkang Yang, Chen Change Loy, and Ziwei Liu. Conditional prompt learning for vision-language models. In *CVPR*, pages 16816–16825, 2022. 2, 3

[88] Kaiyang Zhou, Jingkang Yang, Chen Change Loy, and Ziwei Liu. Learning to prompt for vision-language models. *IJCV*, 130(9):2337–2348, 2022. 2, 3

A. Controllable Feature Compression

Spatially Variable-Rate Feature Compression. As shown in Figure 11, the feature $\boldsymbol{f}$ is input to the encoder g_a and the corresponding compression prompt $\boldsymbol{m}$ is input to the condition network q_a, obtaining the latent variable $\boldsymbol{y}$. Then quantization is performed. The process can be written by:

$$\boldsymbol{y} = g_a(\boldsymbol{f}, \Psi_a), \quad \text{where} \quad \Psi_a = q_a(\boldsymbol{m}),$$
$$\hat{\boldsymbol{y}} = Q(\boldsymbol{y}), \tag{14}$$

where the $\boldsymbol{m}$ denotes compression prompts, and Q denotes the quantizer.

Since the hard rounding quantization operation of Q is non-differential, an additive noise alters quantization [5] during training. As for the inference stage, after real round-based quantization, entropy coding techniques (e.g., Huffman coding and arithmetic coding [70]) can losslessly compress the quantized discrete latent variable $\hat{\boldsymbol{y}}$ if the probability distribution $p_{\hat{\boldsymbol{y}}|\hat{\boldsymbol{z}}}(\hat{\boldsymbol{y}}|\hat{\boldsymbol{z}})$ is given. And we use $\hat{\boldsymbol{y}}$ to denote both $\hat{\boldsymbol{y}}$ of the hard quantized latent variable and $\tilde{\boldsymbol{y}}$ of the noised latent variable for simplicity.

Next, the latent variable $\boldsymbol{y}$ is input into the hyper-encoder h_a and the quantizer Q, obtaining the side-information. This process is formulated as:

$$\boldsymbol{z} = h_a(\boldsymbol{y}),$$
$$\hat{\boldsymbol{z}} = Q(\boldsymbol{z}). \tag{15}$$

Additive noise is also performed for $\boldsymbol{z}$ during training as an alternative of real round-based quantization for differentiability. And entropy estimation of $\hat{\boldsymbol{z}}$ is performed by a learned factorized entropy prior $\boldsymbol{\psi}$, formulated as:

$$p_{\hat{\boldsymbol{z}}|\boldsymbol{\psi}}(\hat{\boldsymbol{z}}|\boldsymbol{\psi}) = \prod_i (p_{z_i|\boldsymbol{\psi}}(\boldsymbol{\psi}) * \mathcal{U}(-\frac{1}{2}, \frac{1}{2}))(\hat{z}_i), \tag{16}$$

where z_i denotes the i-th element of $\boldsymbol{z}$, and i specifies to the position of each signal.

Then the side-information $\hat{\boldsymbol{z}}$ contains both the hyper prior for estimating probability distributions of latent variable $\boldsymbol{y}$ and the conditioned information. It is then fed into the hyper-decoder h_s and the condition generator q_g, which can be written as:

$$p_{\hat{\boldsymbol{y}}|\hat{\boldsymbol{z}}}(\hat{\boldsymbol{y}}|\hat{\boldsymbol{z}}) \leftarrow h_s(\hat{\boldsymbol{z}}),$$
$$\boldsymbol{w} = q_g(\hat{\boldsymbol{z}}), \tag{17}$$

where $p_{\hat{\boldsymbol{y}}|\hat{\boldsymbol{z}}}(\hat{\boldsymbol{y}}|\hat{\boldsymbol{z}})$ denotes the estimated distribution conditioned on $\hat{\boldsymbol{z}}$ and $\boldsymbol{w}$ represents the spatial conditioned information for feature reconstruction. More specifically, the conditional probability distribution $p_{\hat{\boldsymbol{y}}|\hat{\boldsymbol{z}}}(\hat{\boldsymbol{y}}|\hat{\boldsymbol{z}})$ after decoding $\hat{\boldsymbol{z}}$ is modeled by a mean and scale Gaussian distribution, which is:

$$p_{\hat{\boldsymbol{y}}|\hat{\boldsymbol{z}}}(\hat{\boldsymbol{y}}|\hat{\boldsymbol{z}}) \sim \mathcal{N}(\boldsymbol{\mu}, \boldsymbol{\sigma}^2). \tag{18}$$

For feature reconstruction, the decoder g_s and condition network q_s operates on the latent variable $\hat{\boldsymbol{y}}$ and spatial conditional information $\boldsymbol{w}$, which can be formulated as:

$$\hat{\boldsymbol{f}} = g_s(\hat{\boldsymbol{y}}, \Psi_s), \quad \text{where} \quad \Psi_s = q_s(\boldsymbol{w}). \tag{19}$$

Implementation Details. As illustrated in Figure 11, we design the compression framework derived from the Mean & Scale (M&S) Hyperprior model [59] and spatial variable-rate image compression [72]. Residual blocks are used to increase the receptive field and representation capability [16]. Besides, the spatial feature transform (SFT) blocks and spatial feature transform residual block (SFT Resblk) shown in Figure 11 are derived from [72] to modulate features during non-linear transform process.

B. Feature Aggregation Information Selector

The goal of the information selector is to generate compression prompts that adaptively assign importance factors to each location condition on task requirements and feature contents. Since we choose to use the features extracted at stage 1 of Swin Transformer as general features, its network depth is shallow, so the features contain less semantic information. Naturally, we can take use of multi-scale features that contain both detailed spatial layout information and high-level semantic information as input of the information selector to generate more proper compression prompts. Figure 12 illustrates the architecture of the information selector with feature aggregation. Experimental results demonstrate the effectiveness of our proposed simple and lightweight information selector with feature aggregation.

C. Comparison with SOTA ICM Methods

In addition to the comparison with dense prediction tasks, we compare our proposed method with Omni-ICM [26] on CUB-200-2011 [75] fine-grained classification task. Our Prompt-ICM can achieve far superior performance than Omni-ICM, which shows that our framework has robustness on both image classification and dense prediction tasks. We infer that the main reason for the failure of Omni-ICM is because the features learned by contrastive learning in [26] cannot transfer well to fine-grained classification tasks. However, our framework uses more general features, and the proposed task-driven prompts can help us better transfer to downstream tasks, thus obtaining a satisfying performance.

D. Extension of Task-Adaptive Prompts

Note that the the task-adaptive prompts in Prompt-ICM is not constrained to any specific prompt tuning techniques.
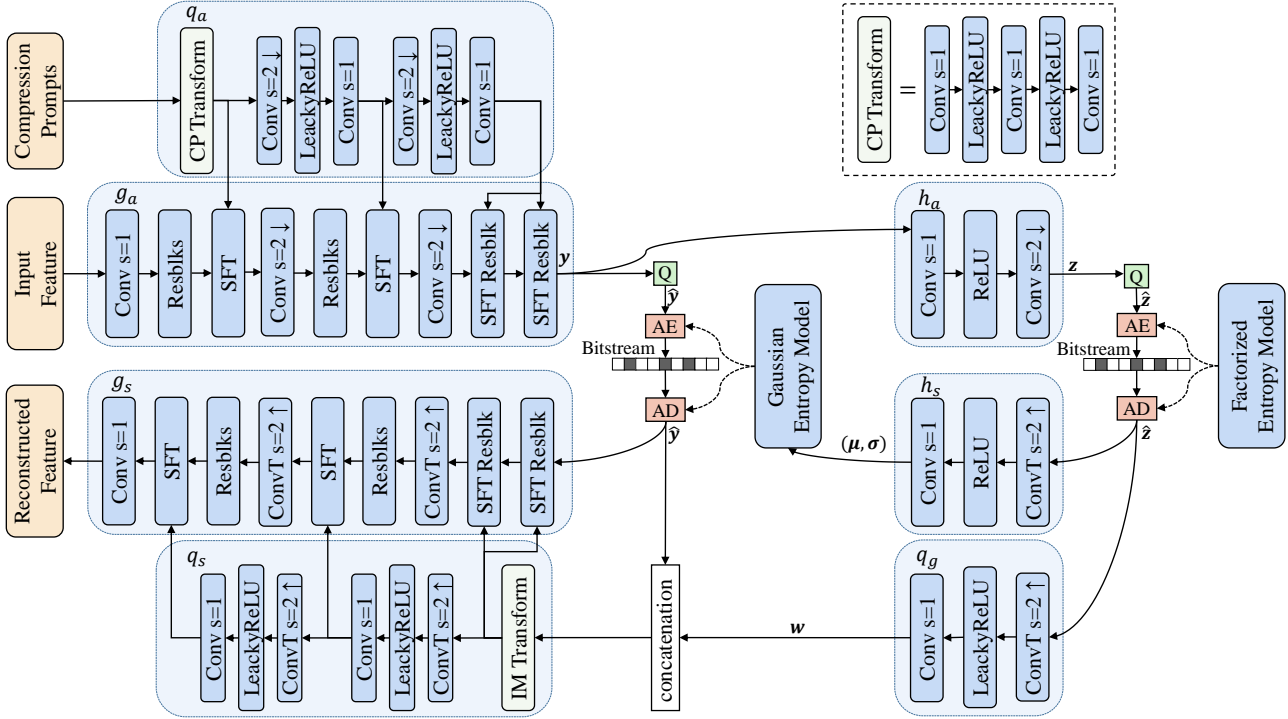
Figure 11. The architecture of our spatially variable-rate feature compression network.
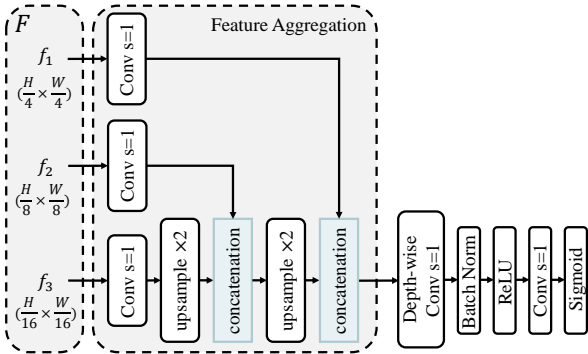

Figure 12. The architecture of information selector with feature aggregation.

Figure 13. Comparison with Omni-ICM [26] on CUB-200-2011 [75].

In the main text, we choose VPT [36] and Pro-Tuning [60] as our instantiation choices. Additionally, we have also instantiated the task-adaptive prompts with CLIP-Adapter [27] to exhibit the versatility of our framework. As illustrated in Figure 14, our Prompt-ICM framework retains its superiority over other methods, which demonstrate the adaptability and compatibility of our framework.

E. Manual Compression Prompts

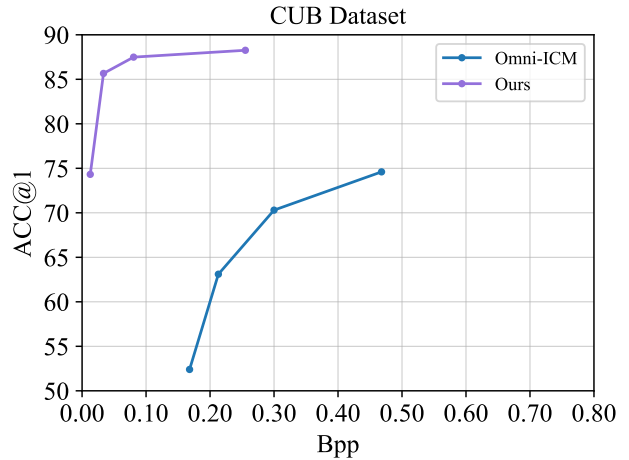The manual prompts mentioned in Section 4.2 of the main text are visualized in Figure 15. Specifically, during the training stage of the codec, to ensure the variety of possible compression prompts, we randomly generate each instance in a mini-batch by using one of the four different ways (1) a uniform map (2) a gradation map between two randomly selected values (3) a kernel density estimation map of a Gaussian mixture with random mean, variance, and a number of mixtures (4) a map consisting of various blocks in a grid manner. During the inference stage, to achieve each point in the rate-distortion curve discussed in Section 4.4.1, we employ uniform maps with a range of [0,
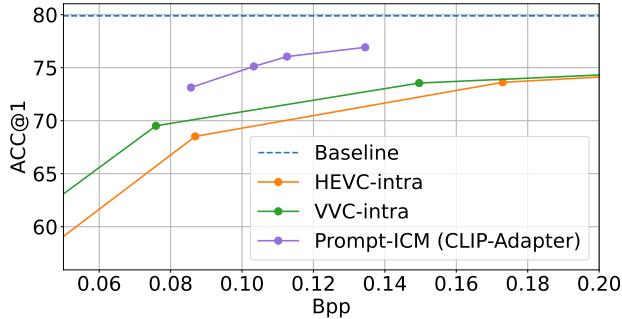
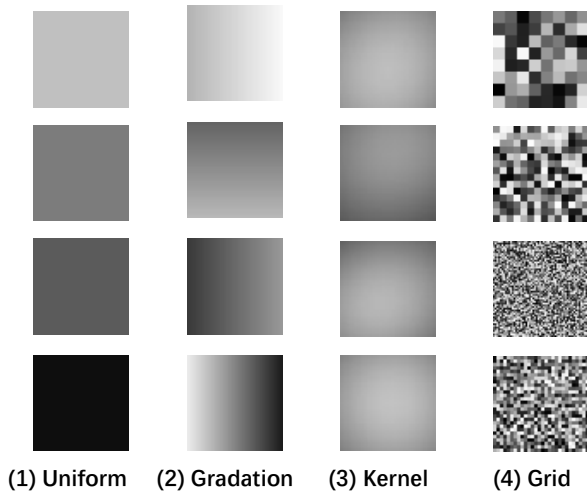Figure 14. Results based on CLIP-Adapter on Stanford-Car.

(1) Uniform   (2) Gradation   (3) Kernel   (4) Grid

Figure 15. Examples of manual compression prompts.

1] as compression prompts, which were set manually.

F. Extension to ViT

Feature Extraction and Feature Compression. We also extend our Prompt-ICM to Vision Transformers (ViT) [22]. More specifically, with a normal ViT consisting of 12 self-attention blocks, we take features extracted at block 6 as the general features. At the downstream transferring stage, the extracted features are fed into the information selector to generate the compression prompts. Then, features and compression prompts are input into the feature compression model. The architecture of the compression model for ViT is almost the same as that of Swin. The only difference is that the stride of all convolutions whose original stride is not 1 is changed to 1, since the ViT features are already 16x down-sampling. As for task-adaptive prompts, we follow the visual prompt tuning (VPT) [36] and take experiments to evaluate the effectiveness on image classification. We conduct experiments on four image classification datasets including CUB-200-2011 [75], Stanford Cars [28], Stanford Dogs [38], and Oxford Flowers [61].

Experimental Results. As shown in Figure 16, Prompt-ICM can extend well to normal Vision Transformer architecture and substantially outperforms the compared methods. It can be inferred that Prompt-ICM are not limited to a certain backbone, and can achieve excellent performance.

Compression Prompts Visualization. For the ViT-based model, Figure 17 shows the compression prompts of the four datasets. As we can see, essential patterns for recognition are allocated by more importance. For example, the heads of birds, cars and dogs are more important to distinguish the image compared to other patterns, while the flower bud is regarded as the key information for flower classification.

G. Limitation

The current state of development in parameter efficient tuning (PET) techniques constrains the upper boundary of Prompt-ICM's performance for dense prediction tasks. Nevertheless, as the PET field advances, this limitation is anticipated to be mitigated.
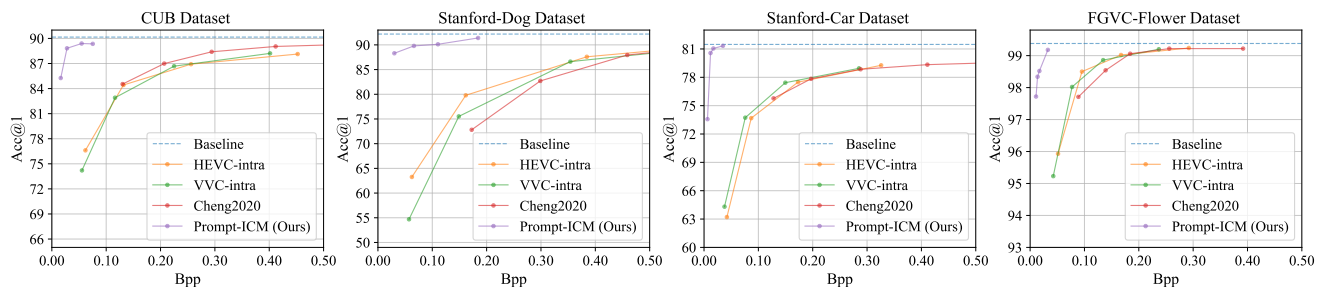
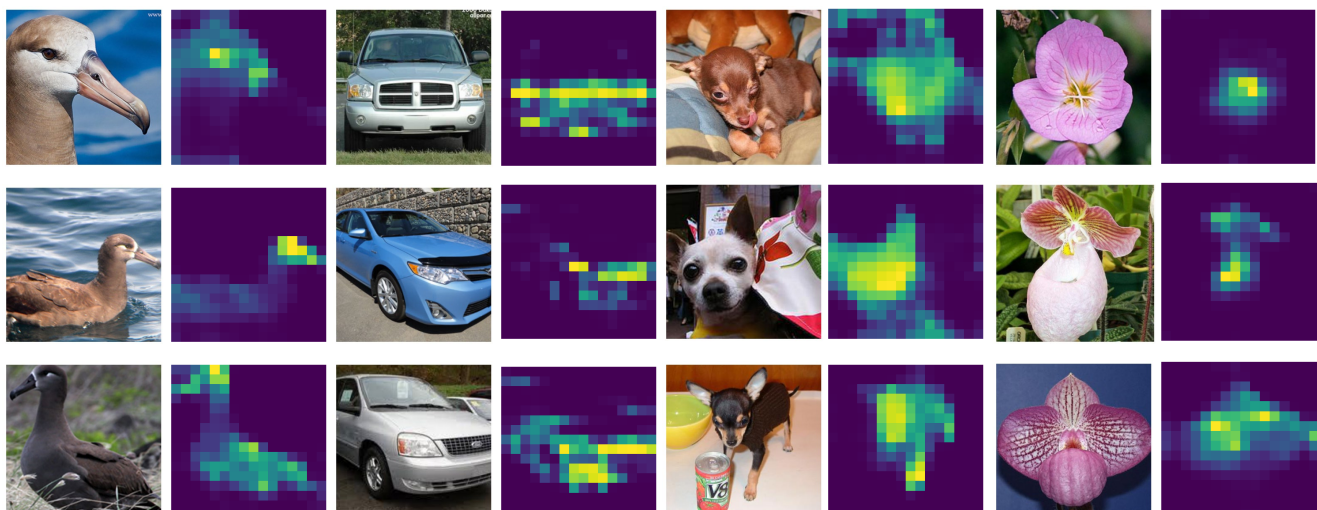Figure 16. Classification results on different datasets under various bitrates by using ViT-B as the backbone.

Figure 17. Visualization of compression prompts by ViT-based Prompt-ICM on different datasets. From left to right, the corresponding datasets are CUB-200-2011, Stanford Cars, Stanford Dogs, and Oxford Flowers. Best viewed in color.